# Short Papers

## Efficient Optical Control of Millimeter Waves in a Slot Line on Semiconductor Plasma Substrate

S. K. Dana, H. Shimasaki, and M. Tsutsumi

***Abstract*—Efficient control of millimeter-waves in a slot line on an Si and GaAs substrate is discussed both theoretically and experimentally. The spectral-domain method is used to estimate the propagation and the attenuation constants in the slot line with the density of the optically induced plasma as a parameter. Experiments in the millimeter-wave range of 35–50 GHz are carried out using high-resistivity Si and GaAs wafers with the dimension of 15 mm $\times$ 30 mm $\times$ 600 $\mu$m. The slot-width could be varied from 0.5 to 2 mm. The attenuation of millimeter waves by over 20 dB can be controlled by optical means using light-emitting diodes with 870-nm wavelength and 68-mW optical power. The experimental results agree considerably well with the theory. The response of millimeter waves with pulsed optical illumination is also examined using a high-power laser diode of 20-W optical power and a pulsewidth less than 100 ns. High-speed response due to optically induced plasma is confirmed for the slot line on GaAs substrate.**

***Index Terms*—GaAs, millimeter waves, optical control, Si, slot line, solid-state plasma.**

### I. Introduction

When photons with energy higher than the bandgap illuminates high-resistivity semiconductors such as silicon (Si) and gallium arsenide (GaAs), solid-state plasma is induced in the semiconductor. The dielectric constant of the optically illuminated semiconductor takes the complex form at microwave and millimeter-wave frequencies, and this can be useful in the design of optically controlled millimeter-wave phase shifters and attenuators, etc. [1]–[5]. With those applications in mind, the optical control of millimeter waves using optically induced plasma waveguides has been studied by the authors, but the efficiency of optical control defined by the ratio of the attenuation of millimeter waves to the applied optical power is low, and it is about 2 dB/100 mW in the waveguides such as image line, rib guide [6], and $H$-guide [7].

This paper treats the optical control of millimeter waves in a slot line on optically induced plasma substrate in Si and GaAs wafers [8]. Theoretical and experimental results on the efficient optical control are discussed.

### II. Theory

The geometry of the slot line is shown in Fig. 1. It consists of a slot of width $W$ on a semiconductor substrate of thickness $t$. The loss factor of the substrate $\tan\delta$ is neglected. The slot region is illuminated by light. Optically induced plasma is assumed with thickness $t_p$ and of infinite extent in the transverse direction. Equivalent dielectric constant of the plasma occupied region is expressed as [1], [2]

$$\epsilon = \epsilon_s - \sum_{i=e,h} \frac{\omega_{pi}^2}{\omega^2 + \gamma_i^2}\left(1 + j\frac{\gamma_i}{\omega}\right) = \epsilon_R - j\epsilon_I \tag{1}$$

Manuscript received January 17, 2000.

The authors are with the Department of Electronics and Information Science, Kyoto Institute of Technology, Kyoto 606-8585, Japan (e-mail: dana@dj.kit.ac.jp).

Publisher Item Identifier S 0018-9480(02)00742-1.

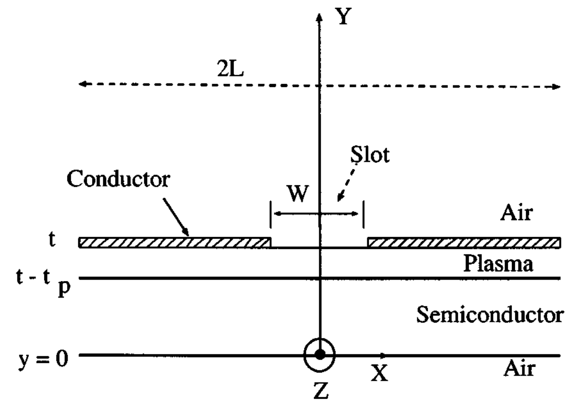


Fig. 1. Geometry of the slot line with optically induced plasma.

where $\epsilon_s$ is the dielectric constant of the host lattice, $\gamma_i$ is the collision frequency, $\omega$ is the radian frequency of the millimeter wave, and $\omega_{pi}$ is the plasma frequency given by

$$\omega_{pi}^2 = \frac{N_p q^2}{\epsilon_0 m_i^*} \tag{2}$$

where $m_i^*$ is the effective mass of electron/hole and $q$ is the electronic charge, $\epsilon_0$ is the free-space permittivity, and $N_p$ is the density of the plasma excited by optical illumination. The imaginary part in (1) governs the millimeter-wave attenuation at low optical power. Thus, optical control of millimeter waves is characterized by attenuation of the wave. The dispersion relation of the slot line is calculated by using the spectral-domain method [9]. All the field quantities are transformed into the Fourier domain, as given by

$$\tilde{f}(K_x) = \int_{-\infty}^{\infty} f(x) e^{jK_x x} dx. \tag{3}$$

The Fourier-transformed Helmholtz equation is given by

$$\left(-K_x^2 + \frac{\partial^2}{\partial y^2} - \beta^2\right)\tilde{\psi} + k^2\tilde{\psi} = 0 \tag{4}$$

where $\tilde{\psi}$ is the scalar potentials in the Fourier domain, $K_x$ is the transform variable in the $x$-direction, and $k^2 = \omega^2\mu\epsilon$. Here, the propagation constant $\beta$ is a complex quantity represented by $\beta = \hat{\beta} - j\hat{\alpha}$ because of the complex form of dielectric constant in (1). The solution of Helmholtz equation in each region of the line gives the scalar potentials from which the Fourier transformed electromagnetic fields with unknown coefficients are obtained. By imposing appropriate boundary conditions at each interface, the algebraic equations are obtained in the matrix form given by

$$\begin{bmatrix} \tilde{J}_x(K_x) \\ \tilde{J}_z(K_x) \end{bmatrix} = \begin{bmatrix} \tilde{Y}_{xx}(K_x,\beta) & \tilde{Y}_{xz}(K_x,\beta) \\ \tilde{Y}_{zx}(K_x,\beta) & \tilde{Y}_{zz}(K_x,\beta) \end{bmatrix} \begin{bmatrix} \tilde{E}_x(K_x) \\ \tilde{E}_z(K_x) \end{bmatrix} \tag{5}$$

where $\tilde{E}$'s are the electric-field components in the slot, $\tilde{J}$'s are the current density components in the conductor, and $\tilde{Y}$'s are Green's ad-

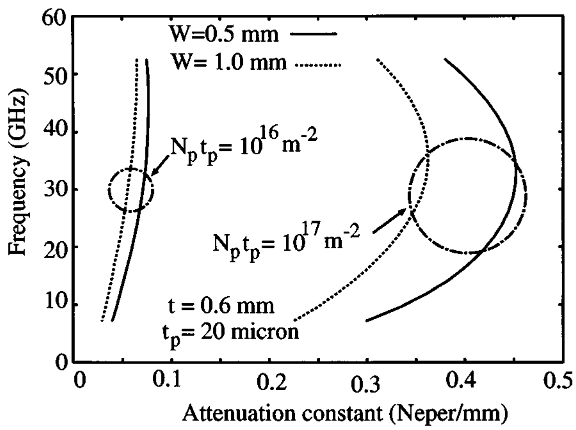


Fig. 2. Attenuation constant $\hat{\alpha}$ for the slot line with the plasma density-thickness product as a parameter.

mittance functions for the slot line. The electric fields in the slot are expressed as the series expansions in terms of basis functions given by

$$\tilde{E}_x = \sum_{i=1}^{I} a_i \tilde{E}_{xi}(K_x) \quad \tilde{E}_z = \sum_{i=1}^{J} b_i \tilde{E}_{zi}(K_x) \tag{6}$$

where $a_i$ and $b_j$ are unknown coefficients. The electric-field basis functions are assumed to be as follows:

$$E_{xi}(x) = \frac{\cos\left[\frac{2(i-1)\pi x}{W}\right]}{\sqrt{1-\left(\frac{2x}{W}\right)^2}} \quad E_{zi}(x) = \frac{\sin\left[\frac{2i\pi x}{W}\right]}{\sqrt{1-\left(\frac{2x}{W}\right)^2}}. \tag{7}$$

Substituting (6) and (7) in (5) and using the scalar product with the electric-field basis functions with both sides of (5) followed by integration over $K_x$ yields the characteristic equation. The dispersion relation is calculated numerically from the characteristic equation. The numerical calculation is carried out for a structure with electric sidewalls separated by a distance $2L$ so that the Fourier integrals can be replaced by discrete Fourier transforms with $K_x = n\pi/L$, where $n$ is an integer [9]. The parameter values used in the calculation are $\epsilon_s = 11.9$, $t_p = 20\,\mu$m, $t = 600\,\mu$m, and the number of basis functions in the expansions of electric field components in (6) is $I = J = 3$.

It is observed from dispersion curves that the real part of the propagation constant $\hat{\beta}$ is not sensitive to the optical illumination, but the imaginary part of the propagation constant $\hat{\alpha}$, as shown in Fig. 2, varies significantly in the range of applied optical power. Thus, millimeter-wave propagation can be controlled by the loss property of the plasma. By comparing with the attenuation constants in image line, rib, and $H$-guide, it is noted that the attenuation constant of the slot line (0.4 Np/mm) is a few times larger for $N_p t_p = 10^{17}/\text{m}^2$ [6], [7]. This is due to the high concentration of electric field at the slot region where the density of optically induced plasma is also high, causing efficient interaction between them. Thus, high-efficiency optical control of millimeter waves can be expected in a slot-line configuration. In this paper, the complex propagation constant has been calculated directly using the spectral-domain method. The real and imaginary parts of the propagation constant obtained here may not be consistent with the result from the Hilbert transform, which has been effective for the estimation of input impedance of the antenna.

## III. Experimental Results

A slot line was fabricated on a high-resistivity Si or GaAs substrate, as shown in Fig. 3. The slot-width $W$ could be varied from 0.5 to 2 mm on an Si or GaAs wafer. To excite millimeter waves in the frequency range of 35–50 GHz, $\text{TE}_{10}$ waveguide transition was used by orienting the waveguide orthogonally to the slot line, as shown in this figure. Light from an array of seven light emitting diodes (LEDs) with an emission wavelength of 870 nm was applied to induce optical plasma in an Si wafer in the slot region. The length of the LED array was 36 mm and the slot line used in the experiment was 30-mm long; thus, the slot line was fully illuminated across its length. The experimental results on optical control of millimeter-wave amplitude is shown in Fig. 4. High-efficiency optical control of millimeter-wave propagation was achieved in this structure. A maximum attenuation of more than 20 dB by applying 68 mW of total optical power was obtained with a wide-frequency response in the slot line on an Si substrate. This corresponds to an efficiency of optical control of over 25 dB/100 mW. However, measured insertion loss was about 10 dB in our setup in the dark state. The transition loss from the waveguide to the slot line may be minimized by using another excitation method such as a nonradiative dielectric waveguide [10] and finline [11]. A maximum attenuation of a wave by 8 dB/cm could be read from Fig. 4, which corresponds to an $N_p t_p$ value of $10^{16}/\text{m}^2$ in the dispersion curve of Fig. 2. This value of $N_p t_p$ is few times less than that in other waveguides reported previously [6], [7]. Thus, the slot-line configuration on an Si substrate as proposed here may find application in the optical control of millimeter-wave attenuators over a wide frequency range using weak optical illumination. It is noted that, in the experiments, plasma was created only in the slot region, but in the model of the slot line in our calculation, uniform plasma density was assumed in the transverse direction. As the electromagnetic field of the millimeter wave is concentrated in the slot and decreases sharply away from the slot region, the experimental results for uniform optical illumination will not be different from our experiment.

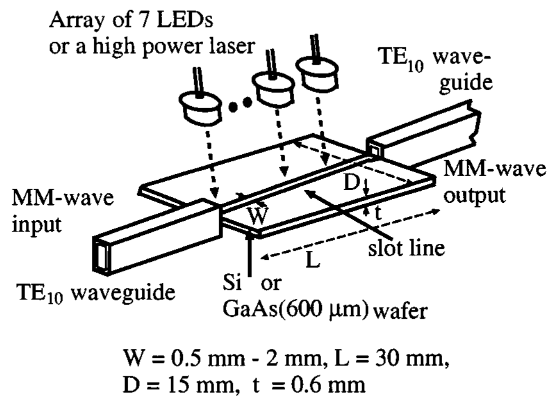


Fig. 3. Geometry of the slot line in the experiment.

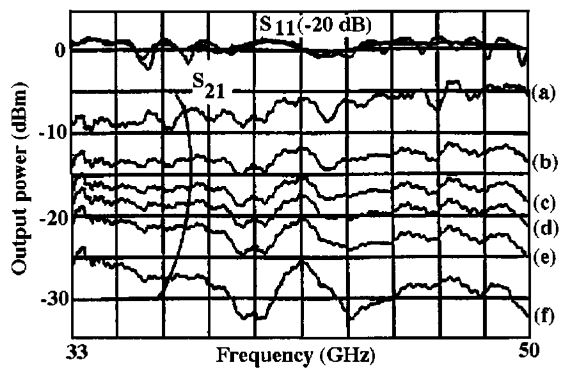


Fig. 4. Optical control of millimeter-wave propagation with seven LEDs; optical power of: (a) 0: dark state, (b) 18 mW, (c) 31 mW, (d) 46 mW, (e) 61 mW, and (f) 68 mW.

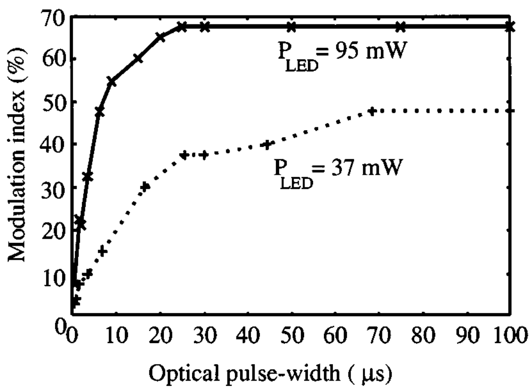


Fig. 5. Pulsed optical response of millimeter wave on Si for two optical input powers.

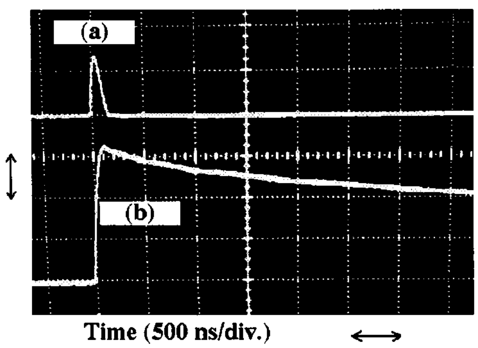


Fig. 6. Millimeter-wave time response for a high-power short optical pulse in an Si substrate. (a) Optical pulse (from laser drive current): 5 V/div. (b) Response of millimeter wave: 10 mV/div.

Next, the time response of optical control of millimeter waves at 40 GHz in the slot line was examined by illuminating with an optical pulse from an array of seven LEDs. The pulsewidth was varied from 500 ns to 100 $\mu$s for two different optical powers. The result is shown in Fig. 5. It was generally observed that the rise time of the millimeter-wave response was less than 0.1 $\mu$s, but the fall time was larger than a few tenths of microseconds. The large fall time is due to the long relaxation time of optical plasma created in the Si material. The modulation index of the millimeter wave due to optical illumination attained saturation when the pulsewidth was 25 $\mu$s with optical power of 95 mW, but for optical power of 37 mW, the modulation index saturated when the pulsewidth was 30 $\mu$s. This is due to the fact that the rise time of the millimeter-wave response decreases as the optical power of the pulse is increased, but the fall time increases with the optical power and, therefore, the saturation characteristics in the output millimeter-wave response vary with the optical power of the pulse.

In the next step, we used a high-power laser with output power more than 20 W and a pulsewidth less than 100 ns with wavelength of 870 nm to control millimeter-wave propagation in the slot line. The response of the millimeter wave at 40 GHz due to a high-power pulsed laser is shown in Fig. 6. A fast rise time of the output, i.e., less than 50 ns, was observed with more than 4 $\mu$s of fall time, thus, the optical control of the millimeter wave is slow.

To overcome the slow response time in the Si substrate, a slot line on GaAs was tested using the same high power laser. The result is shown in Fig. 7. In this case, the response was observed to be similar to the laser drive current. The full width at half maximum (FWHM) of both of the laser–current pulse and the output millimeter-wave response were about 90 ns, as shown in the figure. Thus, high-speed response of optically induced plasma was confirmed for a slot line on a GaAs substrate with short plasma relaxation time. It is noted that the relaxation time of the plasma in GaAs is of the order of $10^{-8}$ s and that in Si is of the

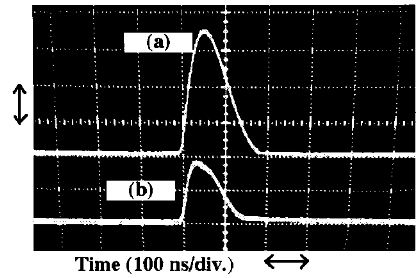


Fig. 7. Millimeter-wave time response for high-power short optical pulse in GaAs substrate. (a) Optical pulse (from laser drive current): 2 V/div. (b) Response of millimeter wave: 5 mV/div.

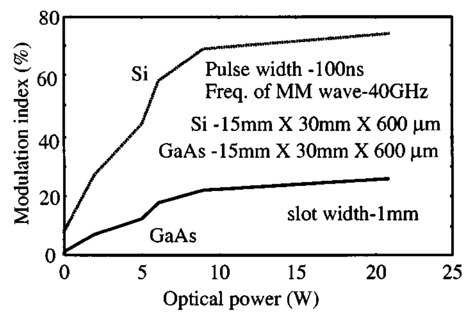


Fig. 8. Modulation index of millimeter wave versus optical power for Si and GaAs substrate.

order of $10^{-6}$ s [12]. The modulation index of millimeter waves due to optically induced plasma using a short high-power pulse was measured for both Si and GaAs and is shown in Fig. 8. A maximum modulation index of 20% was achieved for a GaAs substrate by applying 20 W of optical power with a pulsewidth of 100 ns. The modulation index of the millimeter wave due to optical illumination was insufficient for a GaAs substrate. This is due to the mismatch between the optical wavelength used in the experiment and the optimum wavelength required for plasma creation in GaAs.

## IV. Conclusions

An efficient optical control of millimeter waves in a slot line on an Si and GaAs substrate was discussed both theoretically and experimentally. The spectral-domain method was used for calculating phase and attenuation constants with optically induced plasma density as a parameter. Experiments were undertaken at $Q$-band using a high-resistivity Si and GaAs substrate with the dimension of 15 mm $\times$ 30 mm $\times$ 600 $\mu$m and slot-width in the range of 0.5 to 2 mm. An attenuation of more than 20 dB could be controlled optically with 68 mW of optical power from LEDs at 870 nm. The plasma density-thickness product of $10^{16}/\mathrm{m}^2$ was estimated both theoretically and experimentally. The speed of the optical response was examined for both an Si and GaAs substrate using a high-power pulsed laser with more than 20 W of optical power and less than 100-ns pulsewidth. High-speed response with a modulation index of 20% was observed by applying 20 W of optical power with the pulsewidth of less than 100 ns. The efficient optical control in the slot line has much potential in the design of optically controlled millimeter-wave attenuators and amplitude shift-keying (ASK) modulators at a millimeter-wave band that may replace Schottky diodes currently used.

## References

[1] C. H. Lee, P. S. Mak, and A. P. DeFonzo, "Optical control of millimeter-wave propagation in dielectric waveguide," *IEEE J. Quantum Electron.*, vol. QE-16, pp. 277–288, Mar. 1980.

[2] A. M. Vaucher, C. D. Striffler, and C. H. Lee, "Theory of optically controlled millimeter-wave phase shifters," *IEEE Trans. Microwave Theory Tech.*, vol. MTT-31, pp. 209–216, Feb. 1983.
[3] *IEEE Trans. Microwave Theory Tech. (Special Issue)*, vol. 38, May 1990.
[4] *IEEE Trans. Microwave Theory Tech. (Special Issue)*, vol. 45, Aug. 1997.
[5] W. Platte, "Optoelectronic microwave switching," *Proc. Inst. Elect. Eng.*, pt. J, vol. 132, pp. 126–132, Apr. 1985.
[6] M. Tsutsumi and A. Alphones, "Optical control of millimeter-waves in the semiconductor waveguide," *IEICE Trans. Electron.*, vol. E76-C, pp. 175–182, Feb. 1993.
[7] M. Tsutsumi and Y. Satomura, "Optical control of millimeter-waves in the silicon waveguides," in *Proc. Infrared Millimeter-Wave Conf.*, 1993, p. 539.
[8] S. B. Cohn, "Slot line on a dielectric substrate," *IEEE Trans. Microwave Theory Tech.*, vol. MTT-17, pp. 768–778, Aug. 1969.
[9] T. Itoh, *Numerical Techniques for Microwave and Millimeter-Wave Passive Structures*. New York: Wiley, 1989.
[10] T. Yoneyama, "Properties of guided waves and leaky waves in NRD guide," in *Proc. Asia–Pacific Microwave Conf.*, 1998, pp. 257–264.
[11] C. J. Verver and W. J. R. Hoefer, "Quarter-wave matching of waveguide-to-finline transitions," *IEEE Trans. Microwave Theory Tech.*, vol. MTT-32, pp. 1645–1648, Dec. 1984.
[12] B. G. Streetman, *Solid State Electronic Devices*. New York: Prentice-Hall, 1995.

# A Completely Integrated 1.9-GHz Receiver Front-End With Monolithic Image-Reject Filter and VCO

John W. M. Rogers, José A. Macedo, and Calvin Plett

***Abstract*—A 1.9-GHz monolithic superheterodyne receiver front-end with 300-MHz IF on-chip tunable image-reject filter and voltage-controlled oscillator (VCO) is presented. Two versions of the receiver were fabricated on a 0.5-$\mu$m bipolar process and compared to a previously fabricated version with an off-chip VCO. The two versions are identical, except for the fact that the 2.2-GHz VCO was realized with and without ground-shielded inductors. The receiver that used ground-shielded inductors had a conversion gain of 25.6 dB, a noise figure of 4.5 dB, a third-order input intercept point (IIP3) of −19 dBm, an image rejection of 65 dB, and a phase noise of −103 dBc/Hz at 100-kHz offset. The receiver drew 32.5 mA from a 3-V supply and had a die area of 2.1 mm × 1.7 mm. The local-oscillator–IF isolation improved compared to the previously fabricated front-end with an off-chip VCO.**

***Index Terms*—Inductors, integrated circuit design, MMIC receivers, notch filters, voltage-controlled oscillator.**

## I. Introduction

Superheterodyne receivers are state-of-the-art in mobile communications [1]. A superheterodyne receiver front-end consists of a low-noise amplifier (LNA), an image filter, a mixer, and a voltage-controlled oscillator (VCO), as shown in Fig. 1. An LNA with a very low noise figure (NF) is typically required to enable the receiver to detect very weak signals. Additionally, the LNA must provide sufficient gain to suppress the noise generated by the following stages (image filter and mixer). The image filter is required to suppress the unwanted image frequency, which is located two IFs away from the desired RF [2]. The mixer translates the desired signal from the RF to an IF, usually a lower frequency, for further processing by the receiver back-end. Finally, the VCO allows channel selection of signals in the receive band.

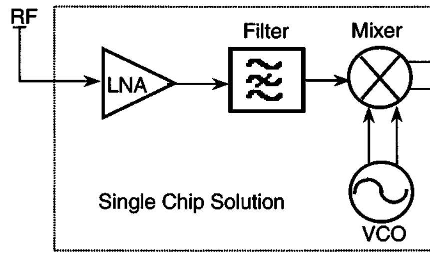


Fig. 1. Block level diagram of a superheterodyne receiver front-end.

Currently, off-chip passive filters, such as surface acoustic-wave (SAW) filters or ceramic filters, are used for image rejection. Recent work has shown, however, that it is possible to integrate the image filter on-chip using either an image-reject mixer [3], [4] or with the use of an image-reject notch filter [5]–[7] It is also typical to use off-chip VCOs or VCOs with off-chip resonators due to the low-$Q$ of on-chip inductors. These filters and VCOs represent the major impediment to raising the level of integration of wireless radios since they cannot be easily implemented monolithically. They also represent a significant fraction of the overall cost of the receiver front-end.

To avoid the cost and complexity of going off-chip between individually packaged components, it is desirable to integrate as many components as possible. Previously it has been shown that it is possible to integrate the image filter on-chip. In this paper, the receiver previously presented in [5] is expanded to include a VCO. This work demonstrates that it is possible to integrate a superheterodyne receiver front-end (LNA, on-chip image filter, and mixer) with a VCO without impacting its performance. Further, the VCO's performance is shown to be improved by the use of inductors with a slotted ground shield that improve their $Q$. The result of this study is an RF front-end with no off-chip components, except for the input matching elements (only one series inductor).

## II. Circuit Building Blocks

An integrated superheterodyne receiver front-end containing an LNA, an image-reject filter, and a mixer was previously developed [5]. This receiver front-end was tested with an off-chip local oscillator (LO) (implemented with an RF signal generator).

The purpose of this paper is to further the integration level of the described superheterodyne receiver by integrating the VCO on-chip. This then ensures the minimum number of RF pins, only one RF input and two IF outputs (differential).

The complete schematic of the integrated receiver consisting of an LNA, a tunable image filter, a mixer, and a VCO is shown in Fig. 2. The buffers (emitter followers) at the IF outputs and the dc bias of $Q_1$ and $Q_2$ have been omitted and $I_3$, $I_6$, $I_{15}$, $I_{16}$, $I_{17}$, and $I_{18}$ are shown as ideal sources for simplicity.

The receiver front-end is designed for a 1.9-GHz RF input and a 300-MHz IF. A high-sided LO of 2.2 GHz is selected and the image, therefore, lies at 2.5 GHz, which is rejected by the image filter.

Manuscript received December 10, 2000; revised February 16, 2001. This work was supported in part by the Natural Sciences and Engineering Research Council of Canada and by MICRONET.

J. W. M. Rogers is with SiGe Microsystems, Ottawa, ON, Canada K2B 8J9.
J. A. Macedo is with Research in Motion, Ottawa, ON, Canada K2H 5Z6.
C. Plett is with the Department of Electronics, Carleton University, Ottawa, ON, Canada K1S 5B6.

Publisher Item Identifier S 0018-9480(02)00734-2.